

Design of Smart Composites Based on Polymer and Shape Memory Alloy Powders

H. Hosoda, S. Takeuchi⁺, M. Yamazaki⁺⁺, T. Inamura,
K. Wakashima and S. Miyazaki*

Precision and Intelligence Laboratory (P&I Lab), Tokyo Institute of Technology (Tokyo Tech)
4259-R2-27 Nagatsuta, Midori-ku, Yokohama 226-8503, Japan.

Phone&Fax 81-45-924-5057, Email: hosoda@pi.titech.ac.jp

*Institute of Material Science, University of Tsukuba, Tennodai 1-1-1, Tsukuba, Ibaraki 305-8573, Japan

Phone&Fax 81-298-53-5283, Email: miyazaki@ims.tsukuba.ac.jp

⁺Graduate Students, Tokyo Institute of Technology (⁺⁺now with Toyota Motor Co. Ltd.)

Since many kinds of shape memory alloys (SMAs) including ferromagnetic SMAs possess poor workability and/or ductility in polycrystal state at least, these SMAs except for Ti-Ni are not practically used. In order to improve workability and ductility of SMAs, a new composite composed of polymer matrix and SMA powder (SMAP) dispersoids is proposed and the design concept, mechanical properties and shape memory properties of the polymer-matrix/SMAP smart composites are described. SMAP can be easily fabricated by crushing mechanically since such SMAs are brittle as mentioned the above. Other important features of the smart composite are isotropic mechanical and shape memory properties. The isotropic properties lead to easy shaping and forming, then, the composites can be made by the injection molding method, for example. Some experimental data for epoxy/NiMnGa SMAP smart composites are also presented and shape memory effect of the smart composites was revealed. Besides, it is pointed out that the improvement of shape memory properties is required for the practical use and that the improvement can be achieved by suppressing the deformation of polymer matrix.

Key words: material design, smart composites, polymer, shape memory alloy, powder, NiMnGa

1. INTRODUCTION

Smart materials with sensing, actuating, self-healing and/or other functions are fascinating and widely studied these days. Shape memory alloys (SMAs) are one of representative smart materials due to the shape memory effect and superelasticity. SMAs exhibit the highest work per volume (= force x strain / volume) [1] thus they are now practically and widely applied for various fields. However, the practical SMA is Ti-Ni only. This is because most of other SMAs have some difficulties in mechanical properties such as poor ductility and poor workability (e.g., Cu-base SMAs and NiMnGa), or poor shape memory effect (e.g., Fe-base SMAs). Besides, even in the case of Ti-Ni practical SMA, some problems are also pointed out: (1) a limited actuation temperature, (2) a possibility of Ni toxicity and (3) a limited frequency in motion [2]. In order to break these limitations, our group has a systematic works for new high-temperature SMAs such as Ti-Ni-Pt [3-6] and new biomedical SMAs composed of nontoxic elements [7-11]. Besides, in order to improve actuation frequency and formability, new smart composites composed of polymer and SMA powder or particles (abbreviated as SMAP) have been proposed [12, 13]. In this paper, the new smart composites composed polymer and SMAP are focused, and the latest results related with shape memory effect are described.

2. DESIGN CONCEPT

It is well known that wire-shape SMAs are one of effective reinforcements to improve tensile strength and ductility of metal-matrix composites due to the large shape recovery force of SMAs against applied force

[14-17]. In the fabrication process of these SMA-base composites, prestrained SMA wires are embedded during forming. Some problems of the composites are shaping and forming after synthesis. The composites with complex shape are difficult to be fabricated in this case.

In terms of shaping and forming, isotropic composites are advantageous and thus powder- or particle-like SMAs should be applied for making composites. Kobayashi and co-workers reported a metal matrix composite containing Ti-Ni SMA particles and found good mechanical properties [18]. A schematic fabrication process of SMAP / polymer composites is drawn in Figure 1, and it is clear that the composite is isotropic because of randomly distributed SMAP. Such SMAP/polymer matrix composites have been investigated and both isotropic physical properties and good mechanical properties were confirmed [12, 13].

Due to the shape memory effect of SMAP, the SMAP / polymer smart composites should exhibit shape memory effect in nature. However, the polymer matrix becomes soft and weak at elevated temperature, the composites are easily deformed for the stress relaxation. (The data for softening will be shown.) On the other hand, magnetic actuation is suitable for the smart composites composed of ferromagnetic SMAP such as NiMnGa. This is because (1) heating is not required for the actuation when using ferromagnetic SMAs, (2) polymer matrix enhances ductility even though ferromagnetic SMAs are brittle, (3) shape recovery stress of ferromagnetic SMAs is small and comparable for deformation stress of polymer and (4) SMAP is easily fabricated for ferromagnetic SMAs due to the

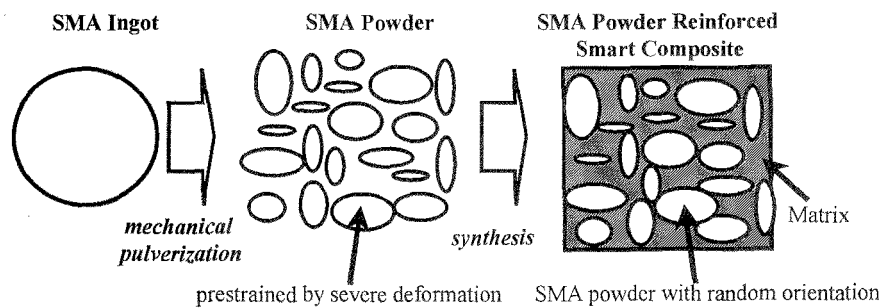


Figure 1 A fabrication method of shape memory alloy powder (SMAP) base smart composites [11].

brittleness. Therefore, in this paper the experimental data for NiMnGa/epoxy matrix composites are focused, and shape memory behavior of the composites was investigated. It should be noted that experiments for magnetic actuation of the composites are now being investigated and thus only the shape memory effect by heating is described in this paper.

3. EXPERIMENTAL PROCEDURE

SMA selected was NiMnGa. The chemical compositions of NiMnGa were 51mol%Ni-26mol%Mn-23mol%Ga (abbreviated as 51NiMnGa) and 54mol%Ni-21mol%Mn-25mol%Ga (abbreviated as 54NiMnGa). These NiMnGa alloys were designed to be martensite phase at room temperature (RT) by considering the relationship between M_s and c/a [19, 20]. The alloys were made by arc melting method with W electrode in Ar-1% H_2 using high purity elements of 99.99%Ni, 99.9%Mn and 99.999%Ga. The alloys were homogenized at 1273K for 3.6ks in vacuum followed by an ordering treatment at 1073K for 3.6ks in vacuum [21]. Then, the alloys were crushed mechanically with the grain size smaller than $150\mu\text{m}$ followed by annealing at 1073K for 900s. The powder fabricated was observed by a scanning electron microscope (SEM) to identify the morphology of the powder. Simultaneous thermogravimetry (TG) and differential scanning calorimetry (DSC) were performed with a heating/cooling rate of 10K/min in Ar with a magnetic field using Netzsch STA449 Jupiter. Conventional θ -2 θ X-ray diffraction analysis (XRD) at RT was performed using Rigaku RINT2000 with $\text{CuK}\alpha$ of 40kVx40mA from 20 to 120 degrees in 2θ .

The smart composites were fabricated by mixing NiMnGa SMAP with epoxy matrix. The epoxy used was composed of a base of epoxy resin (Epikote 828) and a curing agent (Tohmide 280-B). The volume fractions of SMAP were changed from 0% to 50%. The smart composites were mixed and cured at 353K under the pressure of 10MPa for the duration from 130ks to 173ks. Then, specimens for mechanical tests were made by cut and the damaged surface was removed by polishing. It should be noted that no difference in mechanical properties was detected for the smart composites depending on curing time. Tensile tests and constant stress test during thermal cycles were performed by Shimadzu SG-3961-1 and Netzsch DMA 242C. The gauge sizes of plate-shape samples were 0.9mmx5mmx22mm for tensile tests and

1mmx4mmx10mm for dynamic mechanical analysis (DMA). DMA was carried out in a temperature range from 263K to 323K. The heating/cooling rate of DMA measurement was 1K/min with the multi-frequencies from 1Hz to 20Hz. A static force and a dynamic force were selected from 1N to 8N.

4. RESULTS AND DISCUSSION

4.1 Transformation temperatures

Figure 2 shows a SEM micrograph of 54NiMnGa-SMAP. The size of powder used is less than $150\mu\text{m}$. The morphology of SMAP surface indicates the brittle fracture occurring in mechanical crush for making powder. It should be noted that, for the fabrication of the smart composites, larger powder than $150\mu\text{m}$ and smaller powder than $75\mu\text{m}$ were eliminated for the uniformity of the composites.

The apparent phases of both NiMnGa-SMAPs at RT are the martensite phases identified by XRD analysis. Transformation temperatures (M_s , M_f , A_s , A_f and T_c indicating forward martensite transformation start and finish temperatures, reverse martensite transformation start and finish temperatures and Curie temperature) obtained by TG-DSC are listed in Table 1. It was clear that austenite transformation finish temperature (A_f) is higher than RT for each SMAP. Based on these results, the apparent phases of both NiMnGa SMAPs fabricated

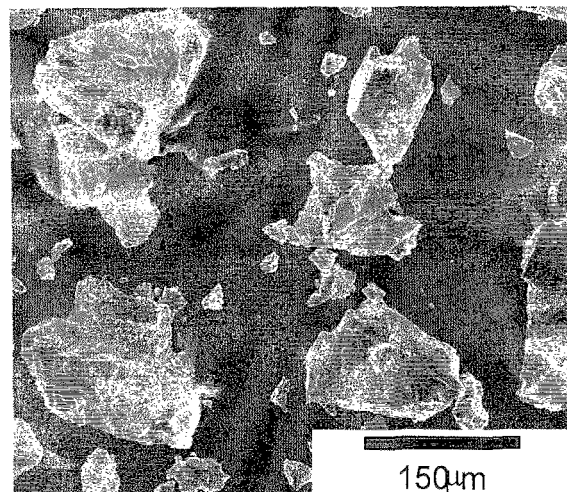


Figure 2 SEM micrograph of 54NiMnGa SMAP.

were mainly martensite phases at RT. It was also found that martensitic transformation temperatures of the smart composites are similar to those of SMAP themselves. This indicates that the existence of polymer matrix does not influence the martensitic transformation temperature of SMAP, partially because the strength and Young's modulus of polymer are low. Therefore, the design of the transformation temperature of such SMAP/epoxy smart composites is much easy in comparison with SMA-wire embedded metal matrix composites.

4.2 Shape memory effect

Figure 3 shows a partial cyclic stress-strain curve of 50vol%-51NiMnGa SMAP/Epoxy at 288K. The arrows in the figure indicate shape recovery by heating over A_f . It is found that the yield stress of the composite is about 3MPa, and that shape recovery occurs by heating. The low yield stress may be due to low flow stress of polymer matrix and/or low stress for reorientation of martensite variants in NiMnGa [22]. The shape recovery strain seems to increase with increasing the number of deformation cycles. However, the specimen was degraded after 7th cycle.

Figure 4 shows the shape recovery strain by heating as a function of applied stress using the stress-strain curves for 50vol%-51NiMnGa-SMAP/epoxy smart composite shown in Fig. 3. Although some scatters exist in data, the shape recovery strain seems to be proportion to the applied stress. The estimated relationship between shape recovery strain and applied stress is expressed to be as,

$$\varepsilon_R = -0.3 + 0.4\sigma \quad (1),$$

where ε_R and σ stand for shape recovery strain (%) and maximum applied stress (MPa), respectively. According to Eq.(1), few shape recovery is expected when applied stress is less than 0.8MPa.

4.3 Strain-temperature relationships for shape recovery

In order to clarify the mechanism of shape recovery of the smart composites, constant stress tests during thermal cycles were carried out under various constant stresses. Figure 5 shows strain of 10vol%-54NiMnGa-SMAP / epoxy smart composite as a function of temperature. The relationships were obtained by DMA where the static force, dynamic force and frequency were selected to be 2N, 1N and multi-frequencies from 1 to 20Hz. It was found that creep deformation appears near and above RT: Such creep deformation is caused by softening of polymer or polymer matrix, and the softening temperature is estimated to be 295K for the epoxy and above 305K for the smart composite. It should be mentioned that the creep resistance of the smart composites increases with increasing the volume fraction of SMAP. However, the smart composites fabricated in this study did not exhibit sufficient creep resistance at elevated temperature.

By considering the results of creep, the following thermal cycle tests were performed in order to evaluate shape recovery of the smart composites. Firstly, a smart composite was cooled down to 280K (below M_s) and deformed at martensite state. After the

Table 1 M_s and T_C of NiMnGa SMAPs fabricated.

SMAP	M_f (K)	M_s (K)	A_s (K)	A_f (K)	T_C^+ (K)
51NiMnGa	252	273	293	308	375
54NiMnGa	267	302	281	314	350

$+T_C$ was evaluated by the slope change in TG curves measured with a magnetic field.

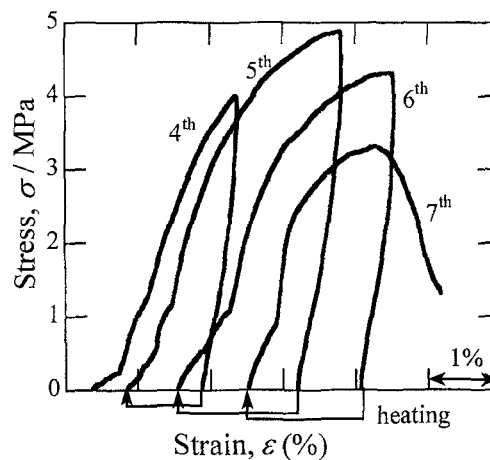


Figure 3 Partial cyclic stress-strain curves of 50vol%-51NiMnGa-SMAP / epoxy smart composite. Note that the numbers shown in the figure stand for the number of cyclic deformation, and that arrows indicate shape recovery by heating. The cycles from 1st to 3rd are removed in this figure for the simplicity.

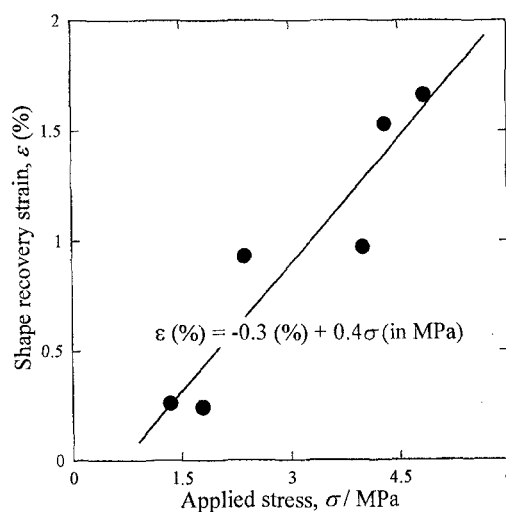


Figure 4 Shape recovery strain as a function of applied stress for 50vol%-51NiMnGa-SMAP / epoxy smart composite.

deformation, the deformed specimen was heated up to 323K (higher than A_s) under the tensile stress being less than 0.1MPa. If the composites possess shape memory effect, shape recovery should be observed. The tensile stress (<0.1MPa) was required to keep straight shape of specimens. Then, finally, the specimen was cooled down to 280K under the same tensile stress being less than 0.1MPa. Since no shape change caused by martensite transformation is expected during cooling, the shape change before and after the test is due to the shape recovery.

Figure 6 shows the results of the thermal cycle tests using 50vol%-51NiMnGa-SMAP/epoxy smart composite where the applied stresses for deformation at low temperature were chosen to be 1, 2, 4 and 5MPa. It is clear for the stress-temperature curve with the applied stress of 1MPa that the specimen was elongated during the cycle and that no shape recovery was observed. The strain increase about 0.1% was caused by creep deformation by holding. On the other hand, when the applied stress increases, some shape recovery was recognized. The shape recovery is started at around 290-300K (near A_s) and finished at around 310-320K (near A_f). Since the shape change was related with the reverse martensitic transformation temperatures (see Table 1), the shape change is concluded to be caused by shape memory effect of SMAP. The shape recovery strain reaches to be 0.15% after deformed by the stress of 5MPa. The nominal strain at 280K caused by the stress of 5MPa was 1.12%. Then, the shape recovery rate, which was calculated to be the shape recovery strain divided by the nominal strain, was 13% ($=0.15\% / 1.12\%$). If the creep deformation around 0.1% is eliminated, the shape recovery rate is calculated to be 22% ($= (0.15\%+0.1\%) / 1.12\%$). Higher shape recovery strain is now being obtained by controlling martensitic transformation temperatures and by selecting much proper polymer as a matrix [23]. However, the shape recovery rate is still less than 30% at present time. Then, improvement of shape memory effect is required for the practical use of the smart composites, and the improvement should be achieved by suppression of plastic deformation of polymer matrix.

5. SUMMARY

For the development of shape memory materials especially for ferromagnetic SMAs, new smart composites composed of polymer matrix and shape memory alloy powder (SMAP) are proposed in this paper. The polymer matrix enhances the ductility, forming and shaping dramatically. Then, the material design and shape memory behavior of the NiMnGa-SMAP/epoxy smart composites were described. Since NiMnGa SMA is brittle, the fabrication of SMAP and the smart composite is easy in this case. The transformation temperatures of the smart composites are similar to those of SMAP, therefore, a deviation of transformation temperatures during processing is not necessarily to be taken into account. However, the shape memory properties are much influenced by the deformation of matrix. The maximum shape recovery strain at present time is around 2% for stress-strain tests and the shape recovery rate is around 20% for the

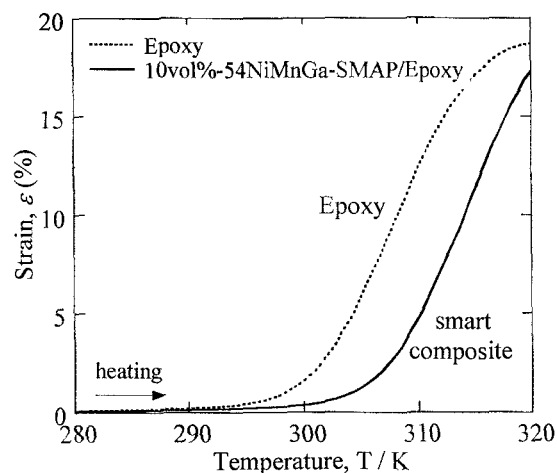


Figure 5 Creep strain caused by constant stress test during heating obtained by DMA. Note that static force is 2N and that dynamic force is 1N with multi-frequencies from 1 to 20Hz. Softening is seen above 295K for the epoxy and above 305K for the smart composite.

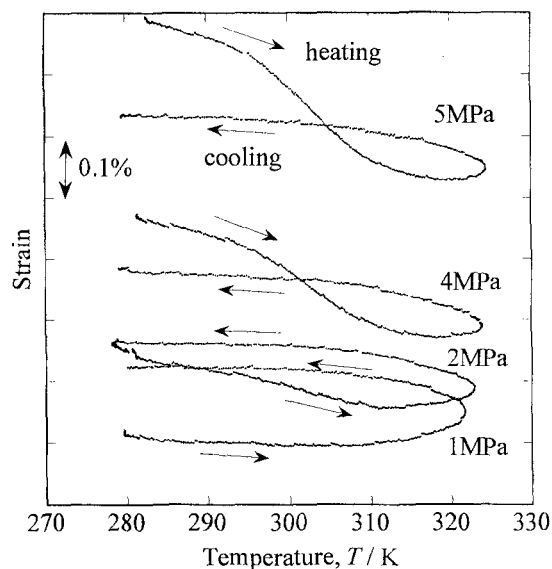


Figure 6 Strain-temperature relationships obtained during thermal cycles for 50vol%-51NiMnGa-SMAP / epoxy smart composite. Note that the specimens were deformed at 280K by the stresses shown in the figure, heated up to 323K under the tensile stress of 0.1MPa, and then cooled down to 280K. Creep deformation was seen above 310K, and shape recovery was recognized near the reverse transformation temperatures listed in Table 1.

constant stress tests during thermal cycles. It is concluded that the SMAP/polymer smart composites are hopeful as new shape memory materials, but that the improvement of shape memory properties is required which must be achieved by suppressing the deformation of polymer matrix.

6. ACKNOWLEDGEMENTS

This work was supported by the Grant-in-Aid for Fundamental Scientific Research (Wakate A (2002-2003)), and partially supported by the 21st COE Program from the Ministry of Education, Culture, Sports, Science and Technology, Japan. The authors thank Dr. Anak Khantachawana of University of Tsukuba for the experimental help.

7. REFERENCES

- [1] P. Krulevitch, A. P. Lee, P. B. Ramsey, J. C. Trevino, J. Hamilton and M. A. Northrup, *J. Microelectromechanical Systems*, 5, 270 (1996).
- [2] H. Hosoda and S. Miyazaki, *Characteristics and Applications of Shape Memory Alloys*, eds. S. Miyazaki, T. Sakuma and T. Shibuya, CMC, Chapter 1, (2001) pp.1-21.
- [3] H. Hosoda, M. Tsuji, M. Mimura, Y. Takahashi, K. Wakashima and Y. Yamabe-Mitarai, *Defect Properties and Related Phenomena in Intermetallic Alloys*, eds. E. P. George, H. Inui, M. J. Mills, G. Eggeler, *Mat. Res. Soc. Symp. Proc.*, 753, BB5.51 (2003).
- [4] M. Tsuji, H. Hosoda, K. Wakashima and Y. Yamabe-Mitarai, *ibid*, BB5.52.
- [5] H. Hosoda, M. Tsuji, Y. Takahashi, T. Inamura, K. Wakashima, Y. Yamabe-Mitarai, S. Miyazaki and K. Inoue, *Materials Science Forum*, 426-432, 2333 (2003).
- [6] Y. Takahashi, M. Tsuji, J. Sakurai, H. Hosoda, K. Wakashima, S. Miyazaki, *Trans. MRS-J*, 28, 627 (2003).
- [7] H. Hosoda, Y. Ohmatsu and S. Miyazaki, *Trans. MRS-J*, 26, 235 (2001).
- [8] H. Hosoda, N. Hosoda and S. Miyazaki, *Trans. MRS-J*, 26, 243 (2001).
- [9] Y. Fukui, K. Kuroda, H. Hosoda, K. Wakashima and S. Miyazaki, *Trans. MRS-J*, 28, 623 (2003).
- [10] K. Kuroda, H. Hosoda, K. Wakashima and S. Miyazaki, *Trans. MRS-J*, 28, 631 (2003).
- [11] H. Hosoda, Y. Fukui, T. Inamura, K. Wakashima, S. Miyazaki and K. Inoue, *Mat. Sci. Forum*, 426-432, 3121 (2003).
- [12] H. Hosoda, S. Takeuchi, K. Wakashima and S. Miyazaki, *Trans. MRS-J*, 28, 647 (2003).
- [13] S. Takeuchi, M. Yamazaki, H. Hosoda, K. Wakashima and S. Miyazaki, *Proc. Annual Meeting of The Japan Society for Composite Materials*, 119 (2003).
- [14] M. Taya, Y. Furuya, Y. Yamada, R. Watanabe, S. Sibata and T. Mori, *Proc. Smart Materials*, ed. V. K. Varadan, SPIE, 373 (1993).
- [15] K. Hamada, J. H. Lee, K. Mizuuchi, M. Taya and K. Inoue, *Materials for Smart Systems II*, eds. E. P. George et al., *Mat. Res. Soc. Symp. Proc.* 459, 143 (1997).
- [16] J. H. Lee, K. Hamada, K. Mizuuchi, M. Taya and K. Inoue, *Materials for Smart Systems II*, eds. E. P. George et al., *Mat. Res. Soc. Symp. Proc.* 459, 419 (1997).
- [17] M. Mizuuchi, K. Inoue, K. Yamauchi, K. Enami and M. Taya, *The Third Pacific Rim Intl. Conf. On Advanced Materials and Processing (PRICM3)*, eds. M. A. Iman et al., TMS, 2, 2051 (1998).
- [18] T. Kobayashi, H. Toda and T. Hashizume, *Trans. MRS-J*, 26, 247 (2001).
- [19] V. A. Chernenko, *Scripta Mater.*, 40, 523 (1999).
- [20] K. Ohi, S. Isokawa, M. Ohtsuka, M. Matsumoto and K. Itagaki, *Trans. MRS-J*, 26, 291 (2001).
- [21] H. Hosoda, T. Sugimoto, K. Ohkubo, S. Miura, T. Mohri and S. Miyazaki, *Intl. J. Applied Electromag. Mech.*, 12, 9 (2000).
- [22] T. Shimada, S. Inoue, K. Koterazawa, K. Inoue, T. Tsurui and K. Murata, *Trans. MRS-J*, 26, 205 (2001).
- [23] H. Hosoda, S. Takeuchi, M. Yamazaki, K. Wakashima and S. Miyazaki, to be published.

(Received October 10, 2003; Accepted March 20, 2004)